Supporting Information

Yamanaka *et al*. 10.1073/pnas.0802556105

SI Materials and Methods

Immunohistochemistry and Evaluation of Microgliosis and Astrogliosis. Floating sections of spinal cords were incubated for 15 min with 0.3% H_2O_2 in PBST to block the endogenous peroxidase, washed, and subsequently incubated with one of the following antibodies diluted in PBST: anti-ChAT (1:200, Chemicon), anti-Iba-1 (1:500, Wako Chemicals, Japan), anti-GFAP (1:4,000, DAKO, Denmark), anti-ubiquitin (1:1,000, DAKO, Denmark), or anti-hSOD1 (1:10,000) overnight followed by biotinylated species-specific secondary antibodies. The staining was revealed by the avidin-biotin complex immunoperoxidase technique (vectastain ABC kit, Vector Laboratories, Burlingame, CA; 1:500 in PBS) and the diaminobenzidine chromogen (Vector Laboratories, Burlingame, CA). Sections were dehydrated and mounted with the toluene-soluble Permount mounting medium (Fisher Scientific).

For evaluating the degree of microgliosis or astrogliosis, 10–12 sections (every 24th 30-μm serial section) per animal representative of the entire lumbar spinal cord were stained with anti-Iba-1 or anti-GFAP antibody, respectively. Different microglial activation stages were defined as follows: stage 0, no microglial activation comparable with a C57BL/6 lumbar spinal cord; stage 1, focal microglial activation; stage 2, mild but diffuse migroglial activation; stage 3, strong activation in the entire section; stage 4, very strong activation in the entire section with some focal aggregation of microglial cells. Different astrocyte activation stages were defined as follows: stage 0, no astrocyte activation comparable with a C57BL/6 lumbar spinal cord; stage 1, focal activation; stage 2, mild activation in the entire section; stage 3, strong activation in the entire section. The level of microglia or astrocyte activation was calculated as the mean of the stages assigned to each hemi-section of the lumbar spinal cord from individual mice.

Cross1	Cross2: Expected Genotypes & Frequencies	Olig⁻ MIT^{146} / Olig⁺ MIT^{170} X Olig⁻ MIT^{146} / Olig⁺ MIT^{170}			Totals
		25% Olig⁺ MIT^{170} / Olig⁺ MIT^{170}	50% Olig⁻ MIT^{146} / Olig⁺ MIT^{170}	25% Olig⁻ MIT^{146} / Olig⁻ MIT^{146}	
SOD1^{G37R} / +; Olig⁺ MIT^{146} / Olig⁺ MIT^{146} X + / +; Olig⁺ MIT^{146} / Olig⁺ MIT^{146}	50% SOD1^{G37R}; Olig⁺ MIT^{146} / Olig⁺ MIT^{146}	8	25	7	40
	50% +/+; Olig⁺ MIT^{146} / Olig⁺ MIT^{146}	6	36	18	60

Fig. S1. Table summarizing the number of chimeras produced. Chimeras with six different genotypes were generated from these embryos. The Olig locus of Olig$^{-/-}$::SOD1^{G37R} chimeras is derived solely from MIT$^{146/146}$. The WT Olig^{+} allele from SOD1^{G37R} mice (Olig^{+} MIT^{146}), Olig^{-} allele from Olig$^{+/-}$ mice (Olig^{-} MIT^{146}), and SOD1^{G37R} allele are highlighted in red, green, and blue, respectively.

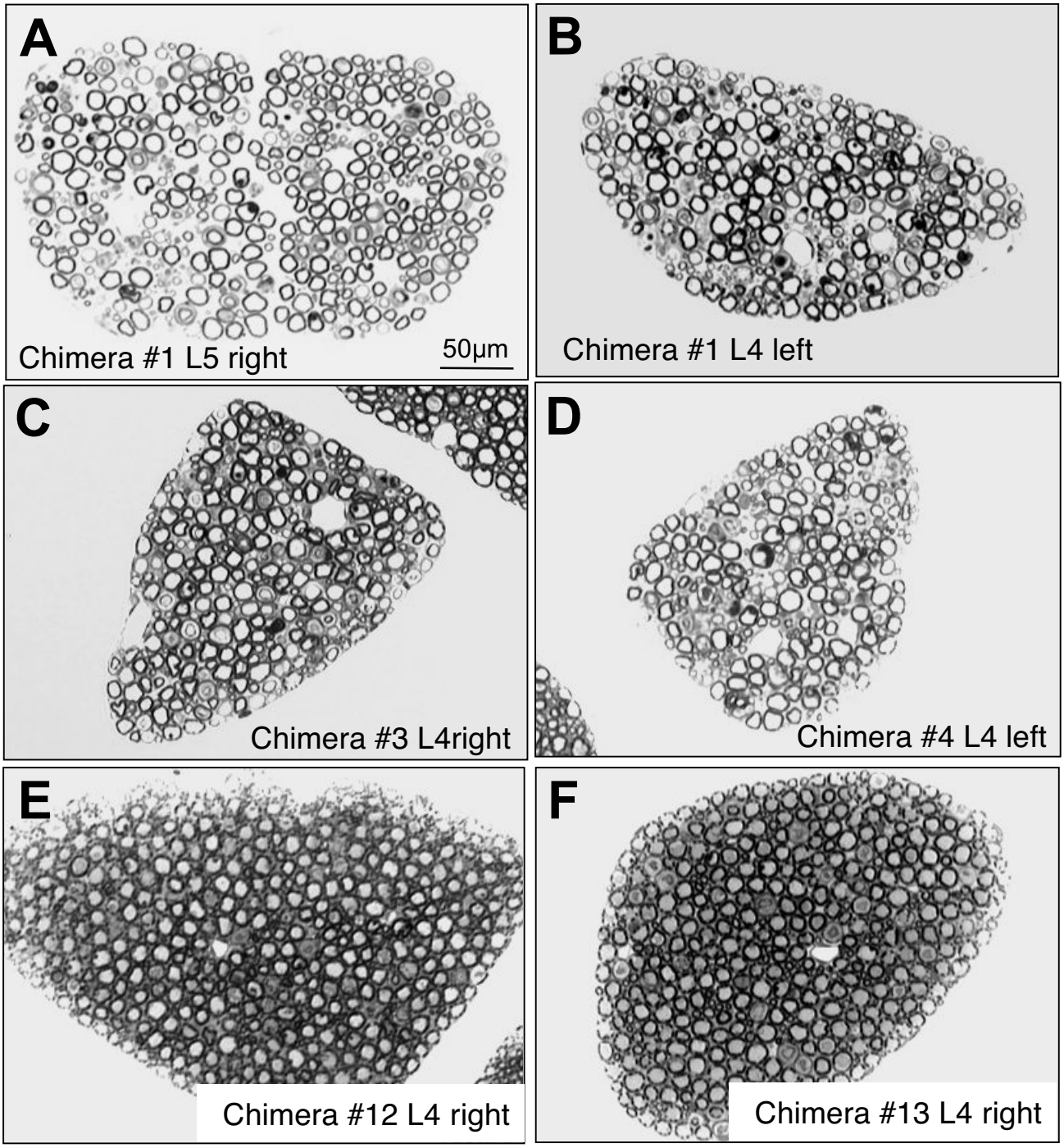

Fig. S2. Representative images of L5 and L4 motor axons of Olig$^{-/-}$::SOD1^{G37R} chimeras (*A–E*) or Olig$^{-/-}$::WT chimera (*F*) which did not develop motor neuron disease. The majority of both L4 and L5 motor axons retain a normal morphology.

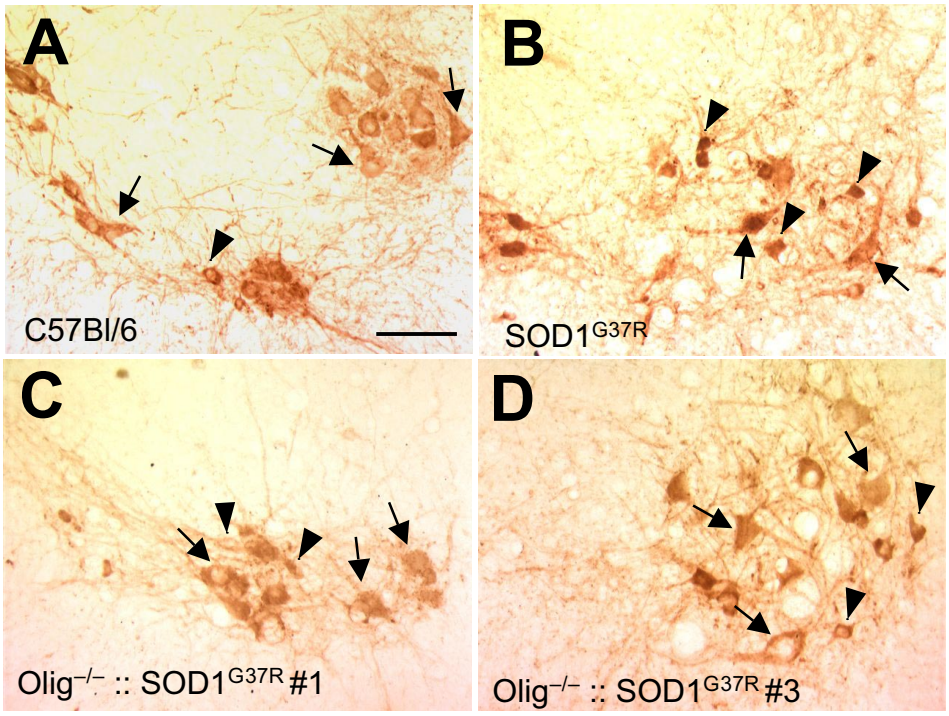

Fig. S3. Representative images of large and small motor neurons quantified in Fig. 3*H*. Shown is immunostaining of lumbar spinal cord sections with the motor neuron-specific anti-ChAT antibody in C57BL/6 (*A*), SOD1^{G37R} (*B*), and Olig::SOD1^{G37R} mice (*C* and *D*). Arrows, large motor neurons; arrowheads, small motor neurons. (Scale bar: 100 μm.)

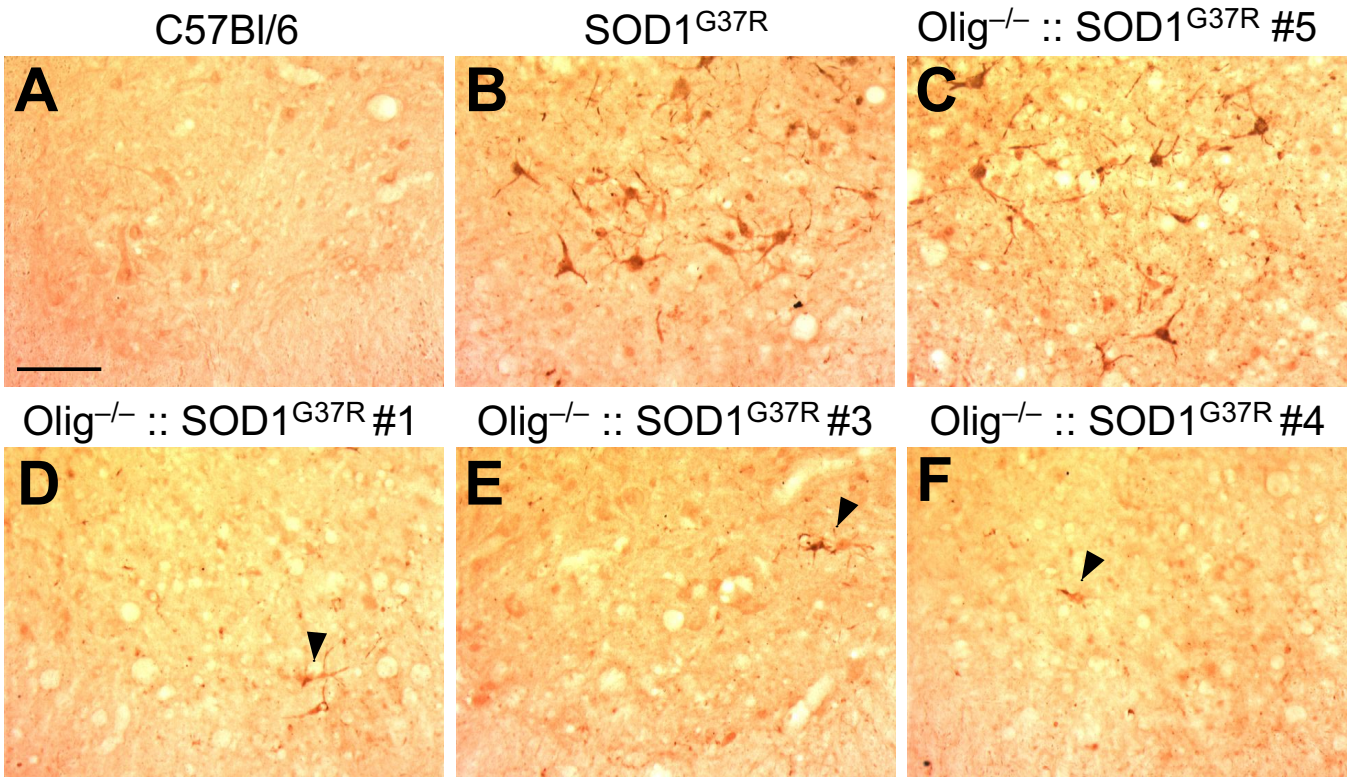

Fig. S4. Reduced ubiquitinated deposits in Olig$^{-/-}$::SOD1^{G37R} lumbar spinal motor neurons. Lumbar spinal cord sections immunolabeled with an anti-ubiquitin antibody from a C57BL/6 (*A*), SOD1^{G37R} (*B*), the Olig$^{-/-}$::SOD1^{G37R} no. 5 that developed ALS (*C*), and Olig$^{-/-}$::SOD1^{G37R} nos. 1, 3, and 4 that did not develop the disease (*D–F*). The numerous ubiquitin-positive motor neurons that are seen in the SOD1^{G37R} mouse are nearly completely eliminated in the Olig$^{-/-}$::SOD1^{G37R} chimeras. (Scale bar: 100 μm.)

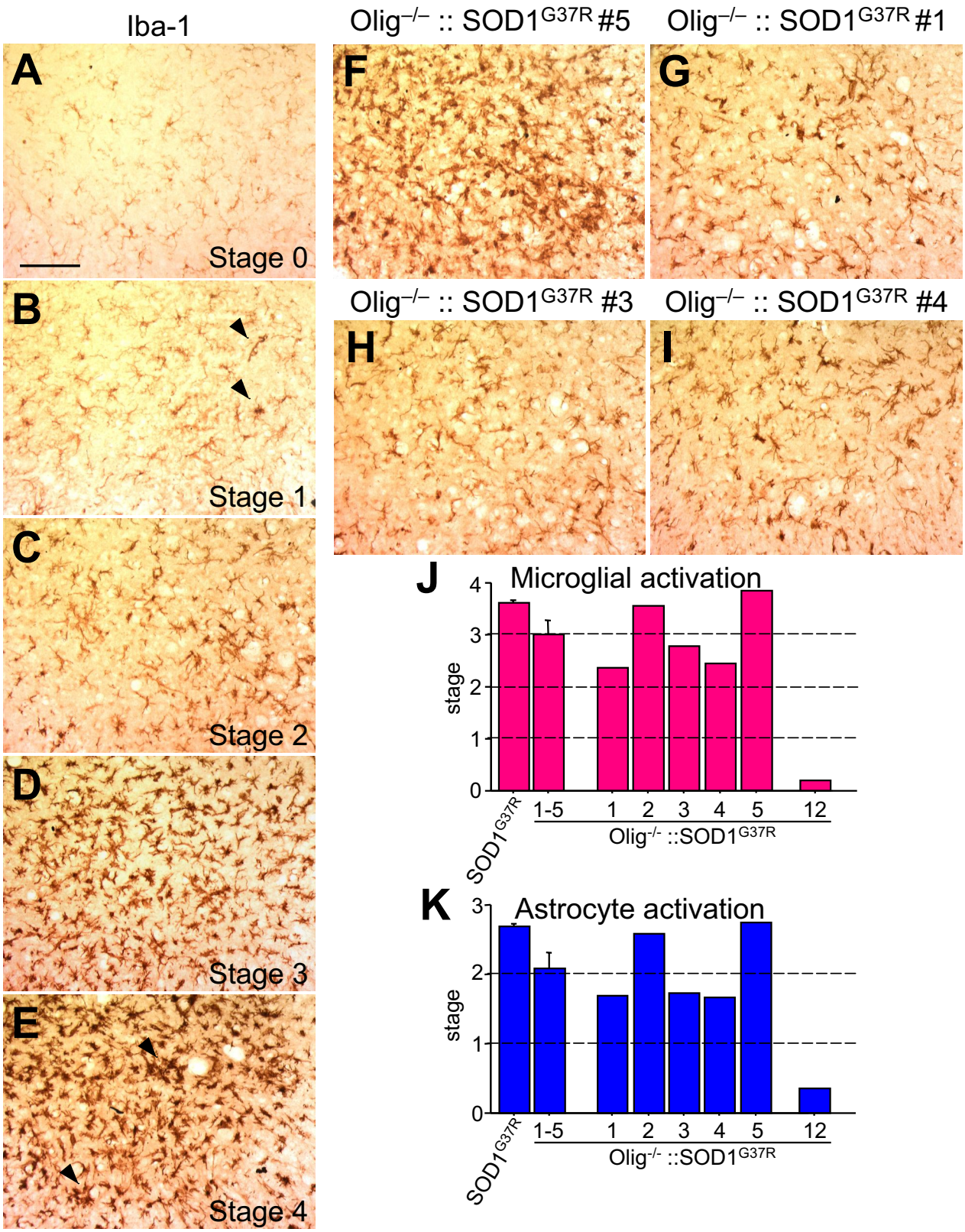

Fig. S5. Olig$^{-/-}$::SOD1^{G37R} mice had initial glial activation. (*A–I*) Microglial cells detected in spinal cord sections using anti-Iba1 antibodies. (*A–E*) Microglial activation stages defined as follows: stage 0, no microglial activation comparable with a C57BL/6 lumbar spinal cord; stage 1, focal microglial activation (arrowheads); stage 2, mild but diffuse migroglial activation; stage 3, strong activation in the entire section; stage 4, very strong activation in the entire section with some focal aggregation of microglial cells (arrowheads). (*F*) Strong microglial activation (stage 3–4) in the Olig$^{-/-}$::SOD1^{G37R} no. 5 that developed ALS disease was seen, whereas there was a milder activation (*G–I*) (stage 2–3) in chimeric mice nos. 1, 3, and 4. (Scale bar: 100 μm.) (*J*) Qualitative measurement of the microglial activation from 10–12 sections per animal derived from all levels of the lumbar spinal cord. (*K*) Astrocyte activation in the lumbar spinal cord detected by immunostaining with anti-GFAP antibodies. Stages of astrocyte activation are as follows: stage 0 (no astrocyte activation) to stage 3 (strong activation), as described in *SI Materials and Methods*. The mean level of microglia and astrocyte activation assigned to each hemisection of the lumbar spinal cord is represented by the bars for each animal or a group of mice.

Movie S1. Chimera no. 13, 65 days old, Olig$^{-/-}$::WT. Abnormal posture of the left hindlimb of this chimera. The abnormal posture was marked during walking or when suspended by the tail.

Movie S1 (MOV)

Movie S2. Chimera no. 4, 40 days old, Olig$^{-/-}$::SOD1^{G37R}. Abnormal posture of the left hindlimb of this chimera. The abnormal posture was marked during walking or when suspended by the tail. Abnormal movement of the left hindlimb was also apparent as was contracture of the left front paw.

Movie S2 (MOV)

Movie S3. Chimera no. 4, 211 days old, Olig$^{-/-}$::SOD1^{G37R}. The clumsiness and abnormal posture of left hindlimb of this chimera did not deteriorate with age (compared with Movie S2 taken at 40 days of age). The mouse showed normal cage activity and escaped from motor neuron disease until 7 months old.

Movie S3 (MOV)

Movie S4. Chimera no. 1, 239 days old, Olig$^{-/-}$::SOD1^{G37R}. Abnormal posture and movement of the right hindlimb of this chimera. The clumsiness and abnormal posture of right hindlimb was observed as early as weaning age. At 8 months old, the mouse showed normal activity in the cage and did not develop motor neuron disease.

Movie S4 (MOV)